17th World Conference on Earthquake Engineering, 17WCEE

Sendai, Japan - September 13th to 18th 2020

COMPARISON OF DAMPING MODIFICATION FACTOR AND METHODS OF ANALYSIS FOR HIGHWAY BRIDGES EARTHQUAKE RESPONSE

F. Dallaire[(1)], X. Robert-Veillette[(2)], M. Barrière[(3)], N. Roy[(4)], J. Proulx[(5)]

[(1)] *P. Eng., Bridge Designer, WSP Canada Inc., Francois.Dallaire@wsp.com*
[(2)] *P. Eng., Project Manager, Commission Scolaire de Montréal (Montreal School Board), RobertVeillette.X@csdm.qc.ca*
[(3)] *Jr. Eng., Bridge Designer, EXP Inc., Melissa.Barriere@exp.com*
[(4)] *Associate Professor, Civil &Building Engineering Department, University of Sherbrooke, Nathalie.Roy@USherbrooke.ca*
[(5)] *Professor and chair, Civil & Building Engineering Department, University of Sherbrooke, Jean.Proulx@USherbrooke.ca*

Abstract

The identification of main dynamic properties is an important step in the analysis of existing structures and in the design of rehabilitation solutions. Three highway bridges located in Eastern Canada, a region of moderate seismicity, are part of a case study to investigate different analysis methods and damping modification factors used for earthquake analysis of small to medium span bridges. The structures were first tested under forced and ambient vibrations. The key dynamic properties (frequencies, mode shapes and viscous damping) were then used to calibrate 3D models. The data acquisition and the model calibration were presented in a previous paper.

In this study, the calibrated models are used to compare three different methods of earthquake analysis: (i) Linear Static analysis; (ii) Non-Linear static analysis; and (iii) Non-Linear Time-History analysis. Damping ratios were varied for the different analysis. The slenderness of the columns was also varied to cover a wider range of vibration frequencies. A comparison of two different damping modification factors was part of the parametric study. The objective was to assess how the selected damping ratios and damping modification factors could influence typical highway bridge earthquake response.

Results obtained with 16 different combinations of models and load cases show that the typical 5 % equivalent damping ratio used in the design of most small to medium span bridges can underestimate the displacement response for structures having low fundamental periods. For an immediate service performance level, where smaller, more frequent earthquakes should not induce damage in a bridge bent, a 5 % equivalent damping ratio will not likely be obtained. Since lower than 5 % damping ratios are frequently obtained during on site vibration tests, recommendations are made to adequately select an equivalent damping ratio and to use proper damping modification factors for reinforced concrete bridge bents in low to moderate seismic hazard areas.

Keywords: *Bridge response; Damping modification factor; Non-linear analysis; Time History analysis; 3D modelling.*

1. Introduction

The identification of main dynamic properties is an important step in the analysis of existing structures and in the design of rehabilitation solutions. Three highway bridges located in Eastern Canada, a region of moderate seismicity, are part of a case study to investigate different damping modification factors used for earthquake analysis of small to medium span bridges. The structures were first tested under forced and ambient vibrations. The key dynamic properties (frequencies, mode shapes and viscous damping) were then used to calibrate 3D OpenSees models [1]. The data acquisition and the model calibration were presented in a previous paper [2]. The focus here is on numerical analysis and damping correction factors.

Different analysis methods can be used to predict the behaviour of bridges subjected to seismic loading. Three well known methods are: (i) linear static analysis; (ii) non-linear static analysis; and (iii) non-linear time-history analysis. One of the important parameters in these analyses is damping, which has a significant impact on the structural responses, but can be misunderstood or misinterpreted by designing engineers.

All structures dissipate energy by damping when they experience a dynamic loading. Elastic viscous damping model is used to model internal friction in materials, while hysteretic damping is related to an inelastic structural behaviour and requires non-linear time history analysis. If an equivalent static method is selected, seismic design spectra provided by design codes consider a 5 % damping ratio. To use these spectra in their initial condition is to assume that the equivalent viscous damping ratio is 5 % for any type of structures. However, measurements made on many bridges suggest that the elastic viscous damping ratio would be between 0.5 % and 2.0 % [2 – 10]. Elastic viscous damping overestimation can reduce the analysis maximum displacements and shear forces. Considering this, some design codes now allow the use of lower than 5% equivalent damping ratio for design.

This paper investigates the effects of the selection of the equivalent viscous damping ratio on the results obtained from linear and non-linear analyses. Three bridges located in Eastern Canada are used in a parametric study to compare different analysis methods (static and dynamic methods) using different elastic viscous damping ratios (from 1 % to 5 %), seismic intensities, loading directions and column slenderness ratios.

2. Damping models

Energy dissipation mechanisms include: elastic viscous damping, hysteretic damping, radiation damping and damping in non-structural elements. The first three types are described below. The latter can be neglected, since non-structural elements are limited in bridges, as opposed to buildings.

2.1. Elastic Viscous Damping

In any dynamic loading, a structure will lose energy due to internal friction forces and micro-deformations in the material. Table 1 shows proposed elastic viscous damping values in design codes from Canada, the United States and Europe. Since bridge bents sustain most deformations during an earthquake, the type of structure mentioned in Table 1 should refer to its material. Note that viscous damping can also be achieved with hydraulic dampers, although this is beyond the scope of this paper.

Table 1 – Suggested Elastic Viscous Damping by Three Different Design Codes

Type of structure	CAN/CSA S6.1:19 (Commentary 5.11.4.1)	AASHTO LRFD (Commentary 4.7.1.4)	Eurocode 8 (Article 4.1.3)
Welded Steel	1 %	1 %	2 %
Bolted Steel	1 %	1 %	4 %
Reinforced Concrete	2 %	2 %	5 %
Prestressed Concrete	2 %	2 %	2 %
Wood	5 %	5 %	—

2.2. Hysteretic Damping

Hysteretic damping can be produced by various non-linear behaviours. In the case of reinforced concrete columns, for example, material deterioration (cracking, spalling) and plastic deformation (in the rebars) cause hysteretic damping. Equivalent viscous damping can be calculated with Equation 1 from Priestley [11], where ξ_0 is the elastic viscous damping and μ is the ductility factor.

$$\xi_{eq} = \xi_0 + \frac{95}{\pi}\left(1 - \frac{1}{\sqrt{\mu}}\right) \% \qquad (1)$$

2.3. Radiation Damping

Radiation damping is caused by dissipation of the bridge motion into its foundation medium (soil, rock). This type of damping requires an approach where soil structure interaction is considered, using a simplified or detailed FEM model for the foundation. The following methods can be used: (i) soil-structure interaction is considered as non-linear with a detailed FEM model of the foundation; (ii) soil-structure interaction is considered as a mass-spring-damper system; and (iii) radiation damping is considered as additional viscous damping (without modelling the soil).

3. Damping Modification Factors (DMF)

As 5 % damping is used in the seismic hazard spectra provided by design codes, some codes and papers propose factors to modify those spectra for different viscous damping values. Examples of such damping modification factors (DMF) are presented in Table 2. Some factors modify the spectral acceleration (R_A) while most factors modify the spectral displacement (R_D). A comparison of these modification factors is provided graphically in Fig. 1 for equations 1 to 10. Note that the R_A DMF value for Equation 5 is used in the graph.

Most equations presented in Fig. 1 are based on studies that evaluated the DMFs for higher than 5 % equivalent viscous damping. Very few studies observed the impact on structures with lower than 5 % equivalent damping. The reason is simple: with classical design objectives of collapse prevention, it was assumed that a structure's response would be non-linear, and therefore the additional equivalent damping from hysteretic damping would surpass the standard value of 5 %. With current Performance Based Design objectives, low-intensity earthquakes may not induce enough damage that would lead to high values of damping and thus the equivalent viscous damping could be lower than 5 %. The graphics of Fig. 1 shows that all equations have a similar impact on damping ratios higher than 5 %, but less so with values lower than 5 %. According to AASHTO [12], Equation 2 should only be used for equivalent viscous damping between 5 % and 10 % if the abutments are designed for sustained soil mobilization, while this is not specified in Canadian Highway Bridge Design Code (CHBDC) [13].

Equation 5 (Newmark & Hall [14]) as well as Equation 11 (Atkinson & Pierre [15]) are different since they consider that the DMF varies with the structure's fundamental period of vibration. In Equation 5, the DMF is given for the constant spectral acceleration, velocity and displacement zone, respectively.

Equation 11 was derived from a table of DMFs values proposed by Atkinson and Pierre [15]. In their paper, ground-motion response spectra relevant for Eastern Canada were compared and average DMF values were then calculated. Since the three bridges in this study are located in the same moderate seismicity region, Equation 11 was selected for comparison in the analysis.

The frequency dependent DMFs from Table 2 (Eq. 5 and 11) are plotted in Fig. 2 (1 – 16 Hz) along with DMFs calculated with equations 2 and 10. All equations are similar for damping ratios from 3 % to 10 %, but the 1 % damping ratio DMF values show notable differences.

Table 2 – List of Damping Modification Factors Proposed in Design Codes and Papers

Source Name	Source Type	Equation	
CHBDC: CSA S6:19 AASHTO: LRFD	Design Codes (Canada and USA)	$R_A = \sqrt[2.5]{\frac{5\%}{\xi}}$	(2)
Eurocode 8	Design Code (Europe, 1994)	$R_A = \sqrt{\frac{7\%}{2\% + \xi}} \geq 0.7\%$	(3)
	Design Code (Europe, 2003)	$R_A = \sqrt{\frac{10\%}{5\% + \xi}} \geq 0.55\%$	(4)
Newmark & Hall	Paper [14]	$\begin{cases} R_A = 1.514 - 0.321 \cdot \ln \xi & (T < T_s) \\ R_V = 1.400 - 0.248 \cdot \ln \xi & (T_s < T < T_L) \\ R_D = 1.309 - 0.194 \cdot \ln \xi & (T > T_L) \end{cases}$	(5)
Shibata & Sozen	Paper [16]	$R_D = \frac{11\%}{6\% + \xi}$	(6)
Tolis & Faccioli	Paper [17]	$R_D = \begin{cases} \sqrt{\frac{7\%}{2\% + \xi}} & (\xi < 5\%) \\ \sqrt{\frac{15\%}{10\% + \xi}} & (\xi > 5\%) \end{cases}$	(7)
Caltrans SDC-2.0	Design Code (California, 2019)	$R_D = \frac{1.5\%}{1\% + 0.4 \cdot \xi} + 0.5\%$	(8)
GB50011	Design Code (China, 2010)	$R_D = 1 + \frac{5\% - \xi}{6\% + 1.4 \cdot \xi}$	(9)
JSSI	Design Guidelines (Japan, 2006)	$R_D = \frac{1.5\%}{1\% + 0.1 \cdot \xi}$	(10)
Atkinson & Pierre	Paper [15]	$R_A = A \cdot \ln(f) + B$ where: $A = -0.087 \ln(\xi) + 0.1648$ $B = -0.277 \ln(\xi) + 1.4416$	(11)

4. Numerical modelling

Three medium span highway bridges were selected for the case study. These structures are described in a previous paper [2], and their main characteristics are presented in Table 3. All bridges have reinforced concrete bents, but with different shapes and heights. The main difference between those bridges is their superstructure.

The three bridges were modelled using OpenSees software [1] and were calibrated using the results of on-site ambient vibration and forced vibration tests [2]. These models were used to investigate the effects of damping and DMFs, using three different analysis methods described below. The column height ratio was varied in the models to allow for a wider range of frequencies to compare in this parametric study. Ratios varied from 4D to 8D, where D is the dimension of the columns in the direction of the analysis. Table 4 shows the 1st transverse and longitudinal frequencies for each of the selected height ratio. Note that only the transverse direction was considered for bridge 2 in this study. Its longitudinal behavior was the focus of another paper looking at the influence of soil-structure interaction on the seismic response (Barrière and al. [18]).

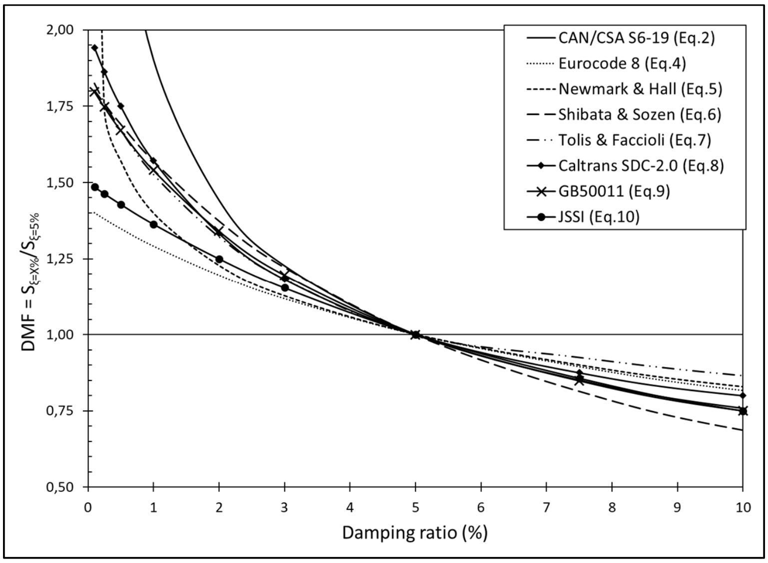

Fig. 1 – Damping Modification Factors: Comparison of Equations 2 through 10

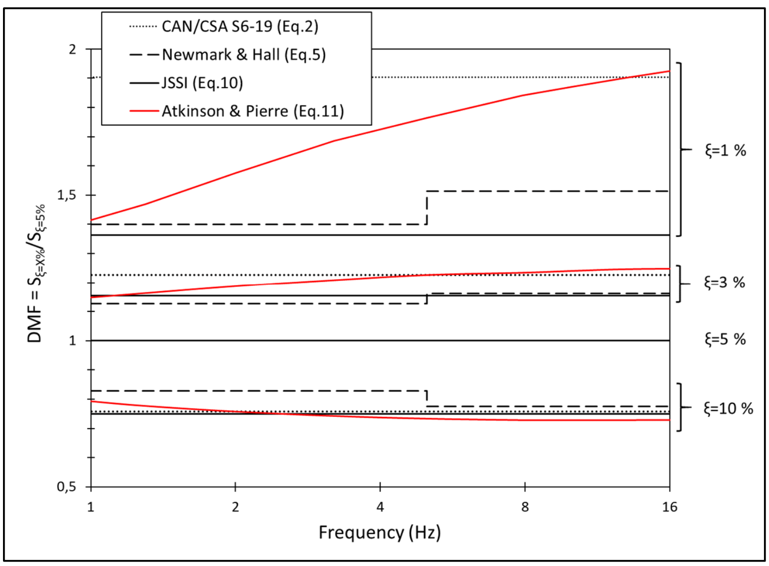

Fig. 2 – Damping Modification Factors: Comparison of Equations 2, 5, 10 and 11

Table 3 – Main Characteristics of Selected Bridges

	Total Length (m)	**Quantity of spans**	**Bent Height (m)**	**Quantity of columns**	**Superstructure type**
Bridge 1	57.0	2	6.18	4	Post-tensioned, cast in place deck and beams
Bridge 2	57.0	2	4.43	3	Conc. deck on welded steel plates girders
Bridge 3	70.1	2	7.32	4	Conc. deck on AASHTO Type V Girders

Table 4 – Computed Frequencies of Elastic SDOF Models

Height ratio	Frequencies of 1st longitudinal and transverse modes (Hertz)					
	Bridge 1		Bridge 2		Bridge 3	
	Longitudinal	Transverse	Longitudinal	Transverse	Longitudinal	Transverse
2.67D	N/A	N/A	N/A	**5.87**	N/A	N/A
4D	**2.38**	**7.69**	N/A	3.74	3.44	2.88
6D	1.32	6.67	N/A	2.72	1.82	**1.68**
8D	0.84	5.88	N/A	2.39	**1.09**	1.19

* A frequency value in **bold** indicates initial height ratio of the columns.

4.1. Type of elements

The bridge bents were modelled using Force-Based Beam-Column elements (*forceBeamColumn*) with *Fiber* sections, using the Cusson-Paultre concrete confinement model [19], adapted to the *Concrete06* material in OpenSees. For the rebars, the *Steel02* material property was used, with a 2 % strain hardening curve. The length of the plastic hinge is calculated with equation 12, proposed by Priestley & al. [20].

$$L_p = 0.08 \cdot L + 0.022 \cdot f_{ye} \cdot d_{bl} \geq 0.044 \cdot f_{ye} \cdot d_{bl} \qquad (12)$$

The numerical integration method selected for the plastic hinge in the *forceBeamColumn* element is a modified two-point Gauss-Radau integration (*HingeRadau*) [21]. This method places integration points at each end and at 8/3 of the hinge length inside the element in order to represent linear curvature distribution. The characteristic length for softening plastic hinges is equal to the assumed plastic hinge length.

Zero-length elements were used for the various elastomeric bearings. The initial horizontal stiffness was calibrated with results of in-situ dynamic tests [2]. A bilinear material was then created to allow a movement with a 1 GPa shear modulus after a horizontal load of 4 % the vertical dead load was reached. All other elements (for the beams and decks, diaphragms, abutments, beam cap, foundations) have linear behaviour.

4.2. Methodology

The models were subjected to two different ground motion intensities. The low intensity earthquakes were selected to obtain an elastic response while the higher intensities were chosen to induce a certain amount of damage in the bent (repairable damage). Two non linear types of analyses (described below) were carried out and compared to a simpler linear static analysis with 5 % equivalent damping ratio. This linear static analysis is typically selected for the type of bridges in this case study (regular, medium span). Damping ratios were varied from 1% to 5%. DMFs were calculated with equations 2 and 11 from Table 2 (CHBDC [13], and Atkinson and Pierre [15], referenced as "CSA" and "A&P" in graphics below, respectively).

4.3. Linear Static Analyses

Linear Static (LS) analysis were carried out as described in the CHBDC [13]. This approach involves a single mode, elastic, forced-based analysis using the spectral accelerations from the Geological Survey of Canada.

4.4. Non-Linear Static Analyses

Non-Linear Static (NLS) analysis were carried out based on the capacity demand diagram proposed by Chopra & Goel [22]. Fig. 3 shows a typical Capacity-Demand-Diagram obtained in the longitudinal direction for Bridge 3 with a height ration of 8D. The step by step methodology presented by Chopra & Goel [22] was then used to create proper inelastic design spectra, as shown in Fig. 3.

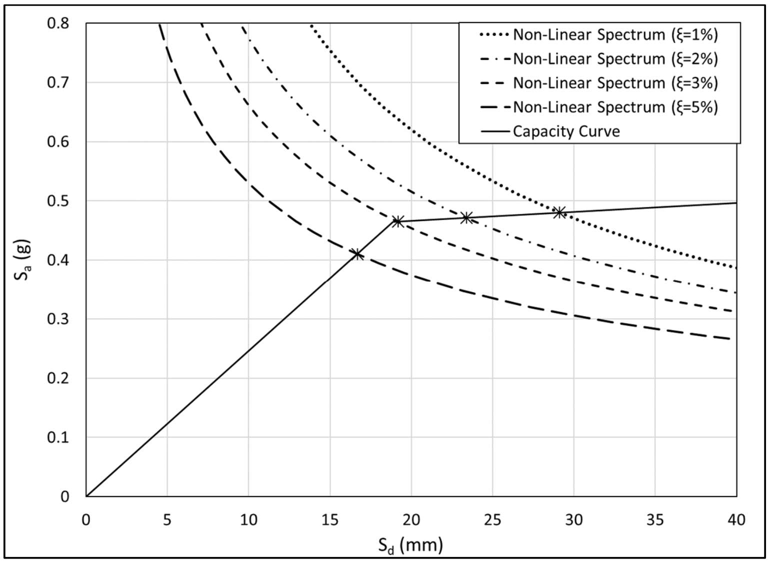

Fig. 3 – Non-Linear Capacity-Demand-Diagram

4.5. Non-Linear Time-History Analyses

Non-Linear Time-History (TH) analysis were carried out using accelerograms artificial earthquake accelerograms generated with the EXSIM software [23] in order to match the Uniform Hazard Spectra published by the Geological Survey of Canada. Fig. 4 shows the selected Design Spectra and the Pseudo-Spectra from the artificial earthquakes. A total of eight earthquakes records were created for each intensity (low and repairable damage) and for each damping ratio (1-5%). The average maximum response obtained for each time history analysis was kept for comparison.

All Time-History analysis were completed using the Newmark integration method with Newton-Raphson algorithm, and Line Search algorithm to solve the non-linear residual equation. Iterative convergence was carried out at each step until a tolerance of 0,01% of the total energy is reached. Rayleigh damping was used, and the damping matrix was recalculated at each step, based on the previous step's stiffness.

5. Results

5.1. Analysis results comparisons

The following four graphs (Fig. 5 to Fig. 8) show the displacements obtained using the five following analysis methods: Linear static with A&P DMF; linear static with CSA DMF, non-linear static with A&P DMF, non-linear static with CSA DMF and non-linear time history. The horizontal line (zero value) in each graph represents the displacements obtained with Linear Static (LS) analysis at 5% equivalent damping ratio (control value). A total of 16 different combinations of bridge models and load cases were used for the five analysis methods. These combinations are the following: three models for both bridges #1 and #3 (three height ratios) using two loading directions (longitudinal and transverse); and four models for bridge #2 using one loading direction (transverse). Table 4 shows the fundamental frequencies associated with each of these 16 combinations. The results in Fig. 5 to Fig. 8 are presented as differences in displacements with respect to the control value, plotted against the period of the 16 bridge model/load case combinations.

Fig. 5 shows results for the reference 5% damping, where both CSA and A&P DMFs are equal to 1.0 (no damping modification). The curves for LS-CSA and LS-A&P are therefore exactly the same, as well as both Non-Linear Static (NLS) curves. This figure shows that the Linear Static method is conservative (higher displacement) when compared to the Non-Linear Time History (NL-TH) analysis, which was expected. The graph also shows that the Non-Linear Static method provides results that are closer to Non-Linear Time-History analysis. The next three figures are presented to investigate the effect of lowering the damping ratio.

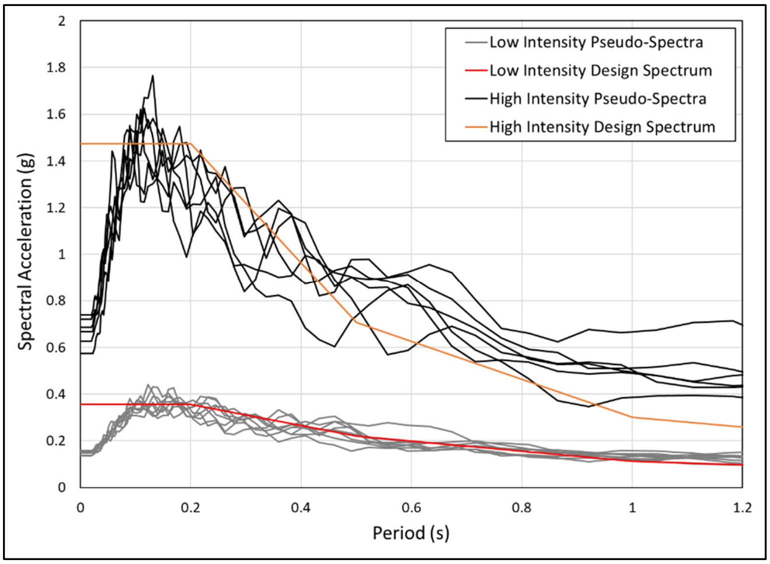

Fig. 4 – Comparison of Design Spectra with Pseudo-Spectra

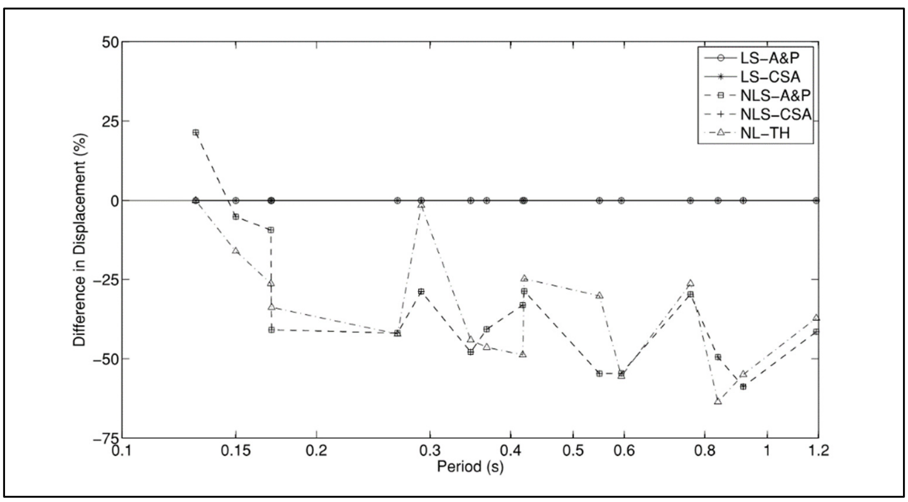

Fig. 5 – Differences in Displacement using 5 % Viscous Damping Ratio

Fig. 6 shows results obtained with 3 % damping ratio, as well as A&P and CSA DMFs. The A&P DMFs are frequency dependent (Fig. 2), therefore the resulting displacement decreases for higher periods. Linear Static analysis is still conservative with 3 % damping when compared to Time History analysis results. Note that Non-Linear Time History results exceed the 5% control value in some cases. Non-Linear Static analysis still provides a good approximation of Non-Linear Time History analysis results.

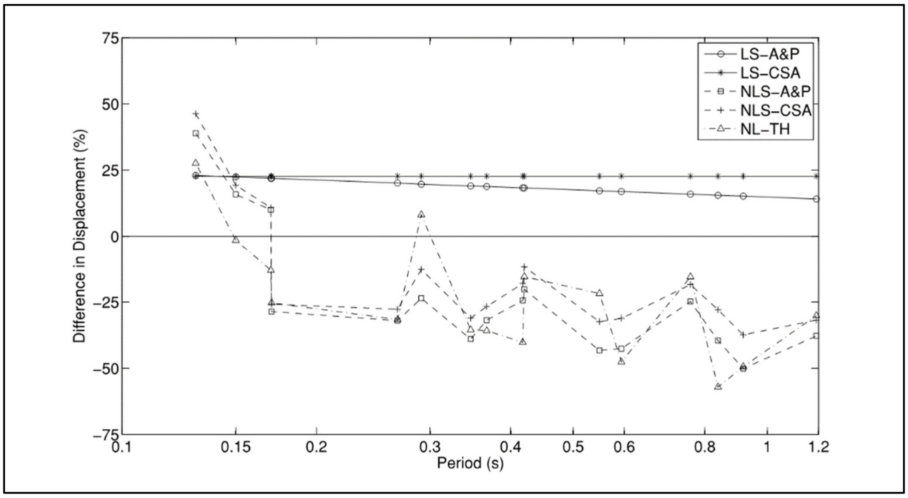

Fig. 6 – Differences in Displacement using 3 % Viscous Damping Ratio

Fig. 7 shows results obtained with 2 % damping. The difference between the frequency dependent A&P DMFs and the constant CSA DMFs increases with lower damping values. This difference is also apparent in the Non-Linear Static analysis curves. The NLS method with A&P DMFs provides results that closely follow the Non-Linear Time History results.

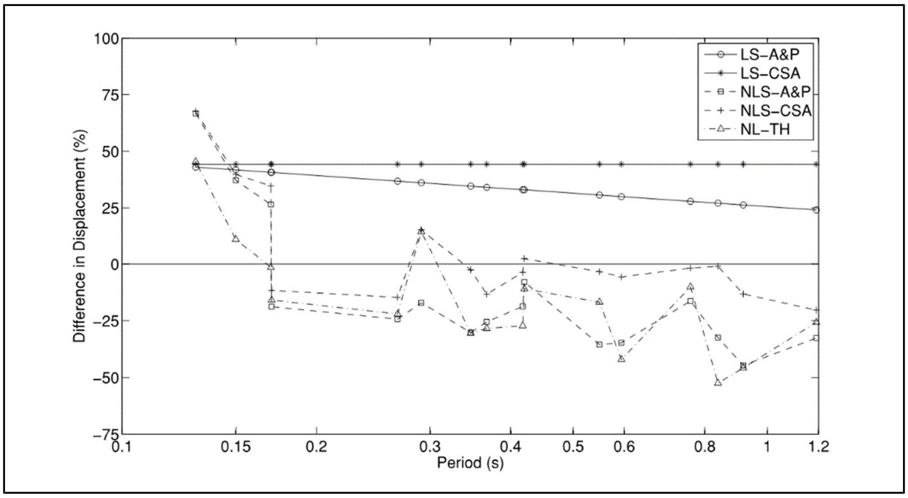

Fig. 7 – Differences in Displacement using 2 % Viscous Damping Ratio

Fig. 8 shows results obtained with 1 % damping ratio. The trends observed in Fig 7 are emphasized here with a lower damping value. Here again, the A&P DMFs combined with Non-Linear Static analysis provide a better approximation of the more complex Non-Linear Time History results. Note that for lower periods, results obtained with NL-TH far exceed the LS 5% damping control value (zero line), which was also observed with 2% and 3% damping.

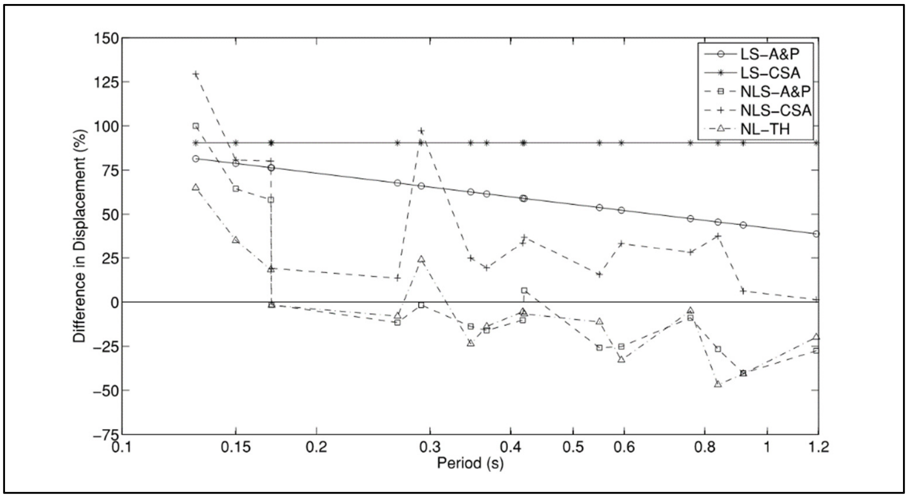

Fig. 8 – Differences in Displacement using 1 % Viscous Damping Ratio

5.2. Non-Linear Time History results comparison with A&P DMFs

Fig. 9 presents individual results (dots) obtained with Non-Linear Time History analysis for the 16 bridge model/load case combinations. These results are shown as ratios of maximum displacements for different damping values with respect to those obtained with 5% damping. The frequency dependent damping modification factors (DMFs) calculated with Equation 11 (Atkinson and Pierre [15]) are also plotted (continuous lines). It can be observed that the A&P DMFs provide an upper boundary and follow the distribution of NL-TH results.

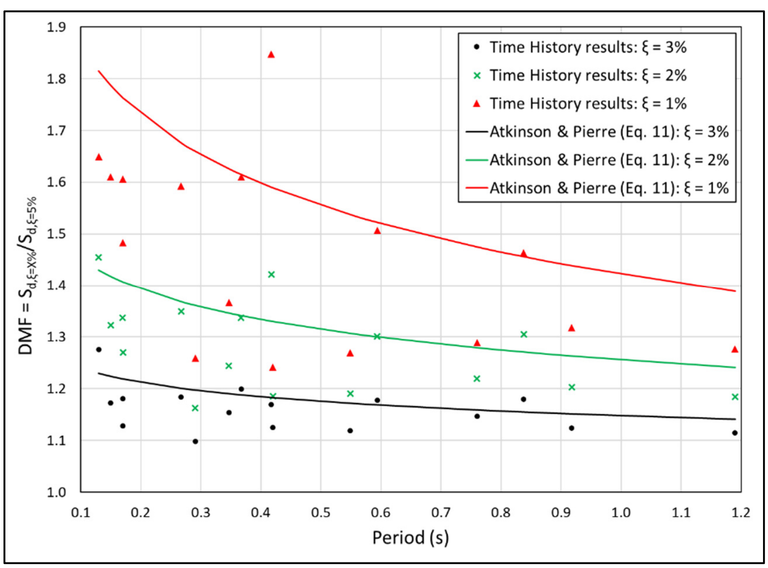

Fig. 9 – Comparison of Non-Linear Time-History analysis results with Equation 11

6. Conclusion and recommendations

This paper presented a review of Damping Modification Factors and analysis methods for highway bridges earthquake responses.

Three bridges were used in a case study where 16 combinations of models and load cases were investigated. The following parameters were studied: column height ratio, loading direction (longitudinal and transverse) and damping ratios. The models were used for earthquake response analysis using three different methods: Linear static, Non-Linear Static and Non-Linear Time History. Two damping modification factors were combined with the static methods (CSA and frequency dependent A&P).

In the scope of a Performance Based Design, low-intensity earthquakes should not induce damage in the structure. This means that no hysteretic damping should be induced, and that the equivalent viscous damping ratio will most likely be lower than 5 %. Failing to consider a lower damping ratio in a static analysis could result in unexpected damage and expensive repair works after a low intensity earthquake, especially for structures with lower fundamental periods. On site dynamic tests carried out on several bridges suggest that the elastic viscous damping ratio used in for low intensity earthquake analysis should be between 0.5 % and 2.0 % [2 – 10]. According to Bimschas [24], the equivalent damping ratio used should never be lower than 2 %, to account for radiation damping in the foundations. Since damping tends to decrease for ageing structures [4, 10], a 2 % equivalent viscous damping ratio seems reasonable for small to medium span bridges with reinforced concrete bents.

Based on the results of this numerical investigation, the frequency dependent A&P damping modification factors (Eq. 11) should be used for low to moderate seimic regions such as Eastern Canada. These factors, combined with Non-Linear Static analysis, provide good estimate of a more time-consuming Non-Linear Time History analyses for values of 5% damping ratio and less.

7. Acknowledgements

The authors would like to acknowledge the financial support of the Quebec Ministry of Transportation (MTQ), the Natural Sciences and Engineering Research Council of Canada (NSERC) and Quebec's FRQNT research fund.

8. References

[1] University of California (2006): *OpenSees Software*, Berkeley, California, United States.

[2] Dallaire F., Robert-Veillette X., Roy N. and Proulx J. (2017): Highway Bridge Damping Evaluation – Forced and Ambient Vibration Testing. *16th World Conference on Earthquake Engineering*, Santiago, Chile.

[3] Billing, J. (1984): Dynamic loading and testing of bridges in Ontario. *Canadian Journal of Civil Eng*ineering 11(4), pp. 833-843.

[4] Salane, H. and Baldwin, J. (1990): Identification of Modal Properties of Bridges. *Journal of Structural Engineering*, 116(7), pp. 2008-2021.

[5] Peeters B. and Ventura C. (2003): Comparative Study of Modal Analysis Techniques for Bridge Dynamic Characteristics. *Mechanical Systems and Signal Processing*, 17(5), pp. 965-988.

[6] Morassi M. and Tenon S. (2008): Dynamic Testing for Structural Identification of a Bridge. *Journal of bridge Engineering*, 13(6), pp 573-585.

[7] Magalhaes F., Cunha A., Caetano E. and Brincker R. (2010): Damping Estimation using Free Decays and Ambient Vibration Tests. *Mechanical Systems and Signal Processing*, 24, pp 1274-1290.

[8] Roy, N., Paultre, P., and Proulx, J. (2010): Performance-Based Seismic Retrofit of a Bridge Bent: Design and Experimental Validation. *Canadian Journal of Civil Engineering*, 37(3), pp. 367-379.

[9] Omenzetter P., Beskhyroun S., Shabbir F., Chen G.W., Chen X., Wang S. and Zha, A. (2013): Forced and Ambien Vibration Testing of Full-Scale Bridges (UNI/578 Report). *Earthquake Commission Research Foundations*, 180 pages.

[10] Li P., Wang Y., Liu B. and Su L. (2014): Damping Properties of Highway Bridges in China. *Journal of Bridge Engineering*, 19(5), paper 04014005.

[11] Priestley M.J.N. (2003): *Myths and Fallacies in Earthquake Engineering, Revisited*. The Ninth Mallet Milne Lecture, 2003. European School for Advanced Studies in Reduction of Seismic Risk, Pavia, Italy, 119 pages.

[12] Imbsen R.A. (2007): *AASHTO Guide Specifications for LRFD Seismic Bridge Design*. Subcommittee for Seismic Effects on Bridges, America Association of State Highway & Transport Officials, 236 pages.

[13] Canadian Standars Association (2019): *S6:19 – Canadian Highway Bridge Design Code*. CSA Group, ISBN 978-4883-1414-8, 1179 pages.

[14] Newmark N. and Hall W. (1982): Earthquake Spectra and Design. *EERI Monograph, Earthquake Engineering Research Institute.*

[15] Atkinson G.M. and Pierre J.-R. (2004): Ground-Motion Response Spectra in Eastern North America for Different Critical Damping Values. *Seismological Research Letter*. 75(4), pp. 541-545.

[16] Shibata A. and Sozen M. (1976): Substitute Structure Method for Seismic Design in R/C. *Journal of Structural Division*, 102(1), pp. 1-18.

[17] Tolis S. and Faccioli E. (1999): Displacement Design Spectra. *Journal of Earthquake Engineering*, 3(1), pp 107-125.

[18] Barrière M., Dallaire F., Roy N. and Proulx J. (2019) Influence of Soil-Structure Interaction on the Seismic Response of Highway Bridges, *12th Canadian Conference on Earthquake Engineering*. Quebec City, Canada

[19] Cusson D. and Paultre P. (1993): Confinement model for high-strength concrete tied columns Rep. No. SMS-9302, Department of Civil Engineering. University of Sherbrooke, Sherbrooke, Quebec (Quebec), Canada.

[20] Priestley M.J.N., Calvi G.M. and Kowalsky M.J. (1996): *Seismic Design and Retrofit of Bridges*. John Wiley & Sons Inc., New York, United States, ISBN 0-471-57998-X, 686 pages.

[21] Scott M. and Fenves G.L. (2006): Plastic Hinge Integration Methods for Force-Based Beam-Column Elements. *Journal of Structural Engineering*, 132(2), pp. 244-252.

[22] Chopra, A.K. and Goel R. (1999): Capacity-Demand-Diagram Methods Based on Inelastic Design Spectrum. *Earthquake Spectra*, 15(4), pp. 637-656.

[23] Atkinson G.M. (2009): Earthquake time histories compatible with the 2005 National building code of Canada uniform hazard spectrum. *Canadian Journal of Civil Engineering*, 36(6), pp. 991-1000.

[24] Bimschas J. (2010): *Displacement Based Seismic Assessment of Existing Bridges on Regions of Moderate Seismicity*. Institute of Structural Engineering, Swiss Federal Institute of Technology, Zurich, Switzerland, 415 pages.